



HAL
open science

Technical Note: An Autonomous Flow through Salinity and Temperature Perturbation Mesocosm System for Multi-stressor Experiments

Cale Miller, Pierre Urrutti, Jean-Pierre Gattuso, Steeve Comeau, Anaïs Lebrun, Samir Alliouane, Robert Schlegel, Frédéric Gazeau

► To cite this version:

Cale Miller, Pierre Urrutti, Jean-Pierre Gattuso, Steeve Comeau, Anaïs Lebrun, et al.. Technical Note: An Autonomous Flow through Salinity and Temperature Perturbation Mesocosm System for Multi-stressor Experiments. 2023. hal-04240387

HAL Id: hal-04240387

<https://hal.science/hal-04240387>

Preprint submitted on 13 Oct 2023

HAL is a multi-disciplinary open access archive for the deposit and dissemination of scientific research documents, whether they are published or not. The documents may come from teaching and research institutions in France or abroad, or from public or private research centers.

L'archive ouverte pluridisciplinaire **HAL**, est destinée au dépôt et à la diffusion de documents scientifiques de niveau recherche, publiés ou non, émanant des établissements d'enseignement et de recherche français ou étrangers, des laboratoires publics ou privés.



1 **Technical Note: An Autonomous Flow through Salinity and Temperature Perturbation**
2 **Mesocosm System for Multi-stressor Experiments**

3

4 **Author list:** Cale A. Miller^{1,2*}, Pierre Urrutti¹, Jean-Pierre Gattuso^{1,3}, Steeve Comeau¹, Anaïs
5 Lebrun¹, Samir Alliouane¹, Robert W. Schlegel¹, and Frédéric Gazeau¹

6

7 1. Sorbonne Université, CNRS, Laboratoire d'Océanographie de Villefranche, 181 chemin du
8 Lazaret, F-06230 Villefranche-sur-Mer, France

9

10 2. Present address: Department of Earth Sciences, Geosciences, Utrecht University, Utrecht,
11 The Netherlands

12

13 3. Institute for Sustainable Development and International Relations, Sciences Po, 27 rue Saint
14 Guillaume, F-75007 Paris, France

15

16

17 **Correspondence to:* Cale A. Miller (c.a.miller@uu.nl)

18

19

20

21

22

23

24

25

26

27

28

29

30

31

32

33



34 **Abstract**

35 The rapid environmental changes in aquatic systems as a result of anthropogenic forcings are
36 creating a multitude of challenging conditions for organisms and communities. The need to
37 better understand the interaction of environmental stressors now, and in the future, is
38 fundamental to determining the response of ecosystems to these perturbations. This work
39 describes an *in situ* mesocosm perturbation system that can manipulate aquatic media in a
40 controlled setting on land. The employed system manipulated ambient water from Kongsfjorden,
41 (Svalbard) by increasing temperature and freshening the seawater to investigate the response of
42 mixed kelp communities to projected future Arctic conditions. This system manipulated
43 temperature and salinity in real-time as an offset from incoming ambient seawater to conditions
44 simulating future Arctic fjords. The system adjusted flow rates and mixing regimes of chilled,
45 heated, ambient seawater, and freshwater, based on continuously measured conditions in a total
46 of 12 mesocosms (1 ambient-control and 3 treatments, all in triplicates) for 54 days. System
47 regulation was robust as median deviations from setpoint conditions were < 0.15 for both
48 temperature ($^{\circ}\text{C}$) and salinity across the 3 replicates per treatment. The implementation of this
49 system has a wide range of versatility and can be deployed in a range of conditions to test single
50 or multi-stressor conditions while maintaining natural variability.

51

52

53

54

55

56



57 **1 Introduction**

58 The persistent burning of fossil fuels since the industrial revolution has radically increased
59 atmospheric CO₂. This has led to an enhanced greenhouse effect resulting in increasing sea
60 surface temperatures (Bindoff et al., 2019). In fjord systems, the confluence of increased fluvial
61 inputs, glacier and permafrost meltwater, stratification and water mass intrusion, as well as
62 increased sea surface temperatures can create periods of extreme physicochemical conditions for
63 nearshore benthic and pelagic marine communities (Bhatia et al., 2013; Poloczanska et al., 2016;
64 Divya and Krishnan, 2017; Bindoff et al., 2019). As ocean changes progress, the need to better
65 understand the effects of combined stressors (e.g., increased temperature and freshening) on
66 nearshore marine communities is essential to understand how community functions and species
67 richness will be affected as assemblages transition to new environmental conditions (Kroeker et
68 al., 2017; Wake, 2019; Orr et al., 2020). Assessing and characterizing the response of organisms
69 and community assemblages to future ocean change is often pursued by conducting *ex situ*
70 experiments, using natural analogues, or space-for-time substitution (when spatial phenomena
71 are used to model temporal changes); however, this can limit the ability to test the range and
72 dynamics of present and future physicochemical conditions (Blois et al., 2013; Rastrick et al.,
73 2018; Bass et al., 2021). The use of *ex situ* experimental systems that manipulate multiple
74 environmental conditions such as temperature and salinity can, thus, be a valuable tool to assess
75 the response to multi-stressors in a future ocean.

76 A principal challenge of conducting an *ex situ* multi-stressors experiment lies within the
77 ability to consistently modulate, replicate, and regulate the experimental conditions in real-time.
78 To date, the majority of experiments conducted on marine organisms and communities have
79 implemented only static changes to physical stressors with a limited capacity to induce



80 variability by either manually changing conditions at set time points or using coarse automation
81 with static setpoints and thresholds (Olariaga et al., 2014; Pansch and Hiebenthal, 2019; Kroeker
82 et al., 2020). Often, this can fail to capture the high frequency variability of *in situ* conditions.
83 When considering the dynamics of physicochemical conditions in nearshore systems that can
84 notably change within tidal cycles (Evans et al., 2015; Hales et al., 2016; Miller and Kelley,
85 2021; Fairchild and Hales, 2021), replication of these environmental scenarios necessitates the
86 development of an autonomous system in order to properly conduct experiments over various
87 periods of time. The advantages of implementing an automated system are that it can overcome
88 the need for capturing and measuring the abundant discrete measurements used to regulate the
89 experimental conditions. This can also remove the need for constant human observation which
90 may not be feasible in the long-term, but may be required to program new regulatory operations
91 and make rapid adjustments to the experimentally manipulated conditions.

92 Here, we describe an autonomous salinity and temperature experimental perturbation
93 mesocosm system (SalTExPreS) that can regulate salinity and temperature in real-time. This
94 system was employed outdoors, along with static light filters to mimic the increase in turbidity
95 and associated irradiance attenuation due to glacial melting to perform a two-month long
96 experiment in Kongsfjorden, Svalbard, exposing mixed kelp communities to future Arctic
97 conditions. The rapidly changing conditions in Kongsfjorden are partly due to intrusion of
98 Atlantic water that increase sea surface temperature, as well as freshening from retreating sea-
99 terminating glaciers and enhanced terrestrial flow from proglacial streams (Tverberg et al.,
100 2019). Such a dynamic multi-stressor environment was ideal for the SalTExPreS deployment.
101 This study focuses on the stability and flexibility of SalTExPreS as an experimental tool to be



102 utilized under extreme and dynamic conditions to test the effects of physicochemical multi-
103 stressors on marine organisms and communities.

104

105 **2 Methods**

106 **2.1 Experimental design**

107 Three experimental treatments representing expected future conditions in Kongsfjorden were
108 considered to examine potential changes in the productivity, survival, and growth of mixed kelp
109 communities present at a 7 m depth in the fjord. This involved manipulating multi-stressor
110 combinations: temperature, freshening, and irradiance (Table 1). The response of communities
111 was determined by conducting weekly assessments of growth and metabolism via closed system
112 incubations (Miller et al., *in prep*). The temperature anomalies used for this experiment represent
113 future Arctic sea surface temperatures projected following scenarios SSP2-4.5 and SSP5-8.5
114 (Meredith et al., 2019; Overland et al., 2019). The salinity offsets were based on correlations
115 between *in situ* temperature and salinity during the 2020 Kongsfjorden summer (Gattuso et al.,
116 2023), weeks 22 to 35 (Fig. A1). This correlation was then used to estimate salinity offsets
117 derived from the temperature offset values extrapolated from a linear fit for treatments 1 and 2
118 (Table 2). In the third treatment, only temperature was manipulated as a way to decouple the
119 multi-stressor system and evaluate a temperature only stress representing coastal areas not
120 affected by glacial melt. The effect of turbidity for treatments 1 and 2 was simulated as a
121 decrease in surface irradiance (i.e., ~ 30 % and ~ 50 % from ambient irradiance at 7 m and
122 corresponding spectra) by the application of a combination of neutral light and spectral filters
123 (Lee© Filters) placed as static fixtures overtop the mesocosms (Fig. S2).



124 Exposed kelp communities were reconstructed in each experimental unit (i.e., a single
125 mesocosm) to represent the species composition found at ~ 7 m depth (Hop et al., 2012; Bartsch
126 et al., 2016; Paar et al., 2019). The biomass of the selected species totaled ~ 4 kg (wet weight)
127 and was composed of *Alaria esculanta* (1 kg), *Saccharina latissima* (1.5 kg), and *Laminaria*
128 *digitata* (1.5 kg). Fauna for each mesocosm was limited to the most abundant organisms found in
129 the field: sea urchins (*Strongylocentrotus pallidus*, *Strongylocentrotus droebachiensis*), snails
130 (*Margarites* spp.), and brittle stars (*Ophiopholis aculeata*) with total biomass weights ~ 400 g for
131 urchins and < 150 g for snails and sea stars at the start of the experiment.

132

133 **2.2 Experimental system**

134

135 Twelve circular mesocosms (3 treatments and 1 control, all in 3 replicates) of 1 m³ (diameter
136 extending from 1.0 at the bottom to 1.2 m at the top, and ~1.2 m high) equipped with a
137 submersible mixing pump, a temperature-conductivity probe, and an optical oxygen sensor (see
138 parts list in Table A1) operated as individual experimental units for the entirety of the 54-day
139 experiment. The determined temperature and salinity offsets applied to treatments 1 – 3 followed
140 a dynamic deviation tracking the control condition. The control condition was designed to
141 represent the actual *in situ* condition in Kongsfjorden at the approximate kelp community depth
142 (7 m). A submersible pump (NPS© Albatros F13T) was deployed at a 10 m depth, 300 m
143 offshore tapped into an underwater intake valve that was plumbed into the header tank of the
144 Kings Bay Marine Laboratory in Ny-Ålesund, Svalbard. Pumped ambient seawater was split into
145 3 sub-header tanks within the marine lab where temperature was manipulated to obtain: ambient
146 seawater, chilled seawater at 0 °C, and warmed seawater at 15 °C. Each sub-header tank was
147 plumbed to supply a constant flow of manipulated fjord water to each mesocosm placed on an
148 open outdoor platform. The control mesocosms received a mix of chilled and ambient seawater



149 to compensate for any potential warming that could occur from transit to the header tank, and
150 finally to the mesocosms. The three experimental treatments received a mix of ambient and
151 warmed water in order to achieve the projected future temperature offsets (Fig 1). Each
152 mesocosm received $0.5 \text{ m}^3 \text{ h}^{-1}$ of seawater in an open cycle which equated to a flow rate of 7 – 8
153 L min^{-1} . The flow was maintained throughout the experiment with the exception of periods when
154 flow to each mesocosm was suspended for 3 h during weekly whole-system incubations for
155 community metabolism determination.

156 The main inflow pipes (ambient, chilled, and warmed) were plumbed in combination
157 with a freshwater tap line (Fig. 1) into a control manifold that mixed the manipulated media
158 regulating flow rates using a continuous monitoring system and a series of controlled valves
159 (Fig. 2). Continuous minutely monitoring of the inflow pressure (pre-mixing) and outflow rates
160 to each mesocosm provided high frequency logging and observation of mesocosm condition.

161

162 **2.3 Parameter regulation**

163 **2.3.1 Temperature and salinity**

164 The control from which temperature and salinity regulation were automated was based on hourly
165 *in situ* readings from the AWIPEV (Alfred Wegener Institute and Institute Paul Emile Victor)
166 FerryBox which is part of the COSYNA underwater observatory (<https://dashboard.awi.de/>). The
167 inlet which is located ~ 400 m from the submersible pump was at 11 m depth. Control conditions
168 were set hourly by the logged COSYNA data, referred to henceforth as the FerryBox. Each
169 treatment condition was retained via manually programmed offsets from the control condition set
170 in the software interface (Section 2.5). The program automatically calculated the salinity offset
171 based on the preset temperature offsets (Table 1). Regulation was maintained via regulation flow



172 valves utilizing minutely measurements of temperature and salinity inside each mesocosm
173 making instantaneous adjustments. This was accomplished using an analog three-way mixing
174 valve for temperature and two-way valve for salinity (BELIMO© R3015-10-S2 with LR24A-SR
175 motor). Each valve was plumbed within the manifold and applied to each mesocosm flow line
176 where its open-position was adjusted (using a PID regulator) to reach the temperature and
177 salinity setpoint value.

178 Accurate temperature and salinity regulation was obtained using a software PID
179 controller on the corresponding Programmable Logic Controller (PLC), in PoE mode
180 (proportional on error). The PID controller measures the difference between the measure and the
181 setpoint (i.e., the error), and calculates how the valve opening should be adjusted by multiplying
182 the error, which is the integral of the error and the derivative of the error, by previously
183 determined coefficients K_p (proportional gain), K_i (integral gain) and K_d (derivative gain),
184 respectively. These coefficients were obtained experimentally using the empiric method of
185 Ziegler & Nichols (1943), and may differ from one condition to another.

186

187 **2.3.2 Pressure and flow regulation**

188

189 Each main inflow line of ambient, cold and warmed seawater had its own pressure regulation
190 system established to maintain equivalent pressure levels, which aided in adjusting the flow rates
191 to the mesocosms. The system consisted of an analog pressure sensor (Siemens© 7MF1567-
192 3BE00-1AA1) and a two-way analog valve (BELIMO© R2025-10-S2 with LR24A-SR motor).
193 A pressure setpoint for all three sensors (K_p , K_i , K_d in software interface) was applied to adjust
194 the valve opening in order to regulate the pressure to the defined setpoint. Each water line with



195 post-mixed seawater flowing to each mesocosm was then manually adjusted and controlled with
196 a hand-crank valve. An analog flow rate sensor (IFM© SV3150) was placed in-line with the
197 piping going to each mesocosm located directly before each hand-crank valve. This provided up-
198 to-date logged flow rate values (updating every 30 sec), which could then be monitored to set
199 incoming flow to each mesocosm.

200

201 **2.4 Automation**

202 The automation was performed using 4 Industrial Arduino-based PLCs (Industrial shields©
203 Mduino-42+), with a single PLC regulating the control and each treatment 1 – 3. Each PLC was
204 responsible for data logging and the regulation of a specific scenario. The PLC regulating the
205 control condition—identified as the Head PLC—was the primary device responsible for
206 communication with the Branched PLCs and the monitoring computer (Fig. A2). All monitoring
207 was performed on a PC Windows application (Section 2.5) and responsible for: (1) reading data
208 received from the PLCs, (2) reading *in situ* data received from the internet, (3) displaying live
209 data, (4) logging data and sending to an FTP server, and (5) sending settings and commands to
210 the PLCs. Communication between the PLCs and the PC was made using http WebSocket
211 protocol on RJ45 ethernet cables, while communication between the PLCs and the conductivity-
212 temperature and oxygen sensors, flow rate sensors, and regulation valves was executed using
213 half duplex RS485 (2 wires) protocol, an analog 4-20mA signal, and analog 0-10V signal,
214 respectively. All PLCs and wired communication lines were housed in an electrical box installed
215 to an IP68 Fibox enclosure with a 400 V (3P+N+E) 32 A security switch. All the automation
216 elements use low tension (12 Vdc or 24 Vdc) through circuit breakers and fuses. The electrical
217 box was protected with a 220 V socket.

218



219 2.5 Software

220 The code for the application was written in C/C++, and developed using Visual Studio
221 community (2019 edition) with the vMicro extension and Arduino 1.8.13. The code uses publicly
222 available Arduino libraries (<https://www.arduino.cc/reference/en/libraries/>) as well as originally
223 designed libraries. All code is available on Github (<https://github.com/purrutti/FACEIT>). The
224 code is divided into two pathways: 'Master.ino' for the Head PLC, and 'Regul_condition.ino' for
225 the Branched PLCs. A description of the main functions applied in the code for programming the
226 system regulation and features are listed in Table A3.

227 The program application has a user-friendly interface designed to allow real-time
228 monitoring and parameterization of regulation processes (Fig. A3). From the interface, the user
229 sets the temperature condition and associated salinity offset, IP address and logging parameters,
230 sensor calibration settings, and pressure setpoints (Fig. A4). The main window displays each
231 mesocosm condition (temperature, salinity, % O₂, and flow rate), their piping connections, a
232 connection status for each PLC informing proper communication, date and time of the last
233 received communication packet from the Head PLC, and the experiment status (e.g., started or
234 stopped). The interface also displays the valve-open percentage along with the pressure setpoints
235 and actual measured value for each main inlet.

236 In addition, the *in situ* data (temperature and salinity) received from the FerryBox is displayed
237 with the date of the last logged value utilized as the programmed real-time condition for the
238 control. Sensor readings of flow rate (L min⁻¹), O₂ concentration (% saturation), salinity, and
239 temperature (°C) are shown for each mesocosm in conjunction with the treatment setpoints (i.e.,
240 temperature, and salinity when relevant). While measured data is stored through the server
241 connection, there is a backup microSD card on the Head PLC that logs data from all mesocosms



242 every 5 sec. The microSD should not be removed before the end of the experiment if possible. If
243 communication fails between the Head PLC and the interfaced computer, data will not be
244 retrieved by the PC during the communication break, but will be retained by the microSD card.

245

246 **2.5.1 Menu bar**

247 Within the menu bar several tabs permit the setup of the project: file, settings, maintenance, and
248 data. Under ‘file’ the system can be manually connected to, or disconnected from, the PLCs.

249 Connection is usually maintained automatically. There is also an exit button that closes the
250 application. The ‘settings’ tab displays the application and experimental setting options (Fig. A4
251 a – c). All the settings of the project are stored on the computer (found in ‘application settings’)
252 that is running the application, which include:

- 253 i. *Master IP address*: The IP Address of the Master PLC (centralizing all the data).
- 254 ii. *Data Query Interval*: Frequency of queries from the application to the master PLC.
- 255 iii. *Data Log Interval*: Number of minutes between logs to file.
- 256 iv. *Data Base File Path*: Directory and base filename of the csv data files.
- 257 v. *FTP Username, Password, Path*: FTP settings for sending the data file every hour.
- 258 vi. *InfluxDB Settings*: For Live Monitoring and local storage of the data.

259 Under ‘experimental settings’, the programmed specificities and regulation of the treatment
260 conditions can be adjusted. This includes programming the setpoints for pressure (all main
261 inflow lines), temperature and the salinity-temperature relational equation (on a different tab
262 selected from dropdown), as well as adjusting the K_p, K_i & K_d coefficients for the regulation
263 (see section 2.3.1). The temperature setpoint is provided by the data received from the ferry-box,
264 however this can be overridden if needed. The « Save to PLC » button sends the values to the



265 corresponding PLC and saves the data, while the « Load from PLC » button loads the settings
266 from the PLC. Loading should be done automatically but this button serves as a way to verify
267 that settings were saved properly. For the purposes of this experiment, the salinity setpoint was
268 calculated based on a delta salinity for treatments 1 and 2 which were derived from the linear
269 relationship with temperature (see section 2.3.1). This can also be overridden if needed by
270 selecting the manual override box.

271 The ‘maintenance’ tab is where sensor calibration and communication ‘Debug’
272 operations can be executed (Fig. A4 d, e). Calibration can be performed for each sensor deployed
273 in each mesocosm, and uses a 2-point calibration for temperature and % oxygen. The salinity
274 calibration is done by setting the conductivity value corresponding to a temperature of 25 °C
275 rather than the *in situ* measured temperature. The conductivity value is programmed as $\mu\text{S cm}^{-1}$.
276 The communication process for sensor calibration is between 5 to 10 seconds. The final option in
277 the menu is the ‘data’ tab which displays the historical and live data. The historical data can be
278 interfaced to an html site if desired.

279

280 **Results**

281

282

283 **3.1 Regulation of the control condition**

284

285 The control condition from which all treatment conditions were offset tracked ambient fjord

286

287 temperature well over the experimental period deviating on average across replicates $< 0.3\text{ }^{\circ}\text{C}$

288

289 (Table 2, Fig. 3). The overall quality of the regulation was based on the ability for the system to

290 read the measured data from the FerryBox, or to be overridden when communication was

291 interrupted and acknowledged by the user. During the experiment, the FerryBox went

292 intermittently offline for 24 % of the time. During these periods the real-time dashboard



293 populated by the COSYNA underwater observatory ceased updating and resulted in a break of
294 communication to the PLCs. There were two main disruptions in the regulation of the control
295 conditions resulting from the main seawater pump failure and a disconnection from the
296 FerryBox. On 2021-07-14 ~21:00 UTC the pump deployed in the fjord suffered a motor
297 malfunction causing a spike in ambient temperatures due to suspended incoming flow of water to
298 the main header tank (Figs. A5, A6). An alternative deep-water pump (90 m) was used as a
299 replacement until the pump at 10 m depth could be repaired on 2021-07-26 13:49 UTC. During
300 this period, the control condition was colder than the target fjord temperature at 7 to 10 m depth
301 by $> 1\text{ }^{\circ}\text{C}$ (Figs. 3, 4) until the proper pump depth was reestablished. The average deviation
302 (Table 2) excluded this period as the control condition was unable to be warmed as only cold and
303 ambient water lines were plumbed to the control condition (see section 2.2). The other instance
304 occurred on 2021-08-24 04:47 UTC when setpoint values did not retain the last FerryBox
305 reading and dropped to $0\text{ }^{\circ}\text{C}$. This issue was quickly resolved ($< 8\text{ h}$) by resetting the PLC.

306

307 **3.2 Temperature and salinity regulation**

308

309 Regulation of the temperature and salinity treatment conditions was maintained for 54 days (i.e.,
310 entirety of the experiment) (2021-07-03 – 2021-08-26) by the SalTExPreS: the entirety of the
311 planned experiment. All mesocosm conditions were held at ambient temperature and salinity for
312 the first 6 days dedicated as an acclimation period before proceeding with an incremental rise in
313 temperature over a 5-day period starting on day 7 (2021-07-10 12:00 UTC). Treatment 1
314 temperature increased by $0.55\text{ }^{\circ}\text{C d}^{-1}$, while treatment 2 and 3 increased by $0.88\text{ }^{\circ}\text{C d}^{-1}$ (Figs. 3,
315 A5). The temperature offsets achieved final values at $\sim 2021-07-15\text{ }21:00\text{ UTC}$, 4 h after the
316 final incremental increase (Fig. 3, A5). Due to technical issues with the incoming FerryBox data,
317 the final salinity offset values for treatments 1 and 2 were reached immediately with the first



318 incremental temperature increase on 2021-07-10 12:00 UTC because the programmed setpoint
319 based on the linear relationship with temperature was set as a manual override (Fig. 4).

320 The regulation of temperature and salinity was well maintained over the duration of the
321 experiment as the difference between the measured and setpoint value was < 0.3 °C and < 0.36
322 salinity across the three replicates per treatment (Table 2). Stochastic periods of deviations that
323 were greater than the mean value (Table 2) was due to various anomalies. In the event of a
324 communication break between the FerryBox and the Head PLC, the system is programmed to
325 automatically retain the last value read. Thus, regulation would be maintained based on this last
326 *in situ* temperature, unless a manual value was programmed as an override. On 2021-08-24 04:47
327 UTC, when connection with the FerryBox was interrupted, the last value was not retained and
328 resulted in strong deviations in the regulation until a manual value could be implemented (Fig.
329 A5). This happened on only one occasion and was resolved by rerunning the program code. The
330 disconnection from the FerryBox was due to interrupted logging by the FerryBox on the
331 COSYNA dashboard (<https://dashboard.awi.de/>), and was not a result of programming
332 miscommunication. The only lasting miscommunication error between the program and PLCs
333 occurred from 2021-07-21 to 2021-07-26 where data logging ceased, however, regulation was
334 maintained. The result was a loss of all measured data during this time period, but resulted in an
335 addition to the programming code which provided a ‘disconnection pop-up window’ henceforth.
336 Connection could easily be reestablished by resetting the master PLC (i.e., pressing the reset
337 button or cycling the power).

338 The salinity regulation for treatments 1 and 2 across replicates experienced a sudden
339 freshening on 2021-08-03 07:30 UTC resulting in an upward shift of the mean offset value (Fig.
340 A5). This event was quickly resolved by a system reset and lasted for only 2 h. Deviations in one



341 mesocosm (1st replicate of treatment 2) occurred intermittently from 2021-07-26 to 2021-08-03
342 due to a recurring communication issue with the treatment 2 branched-PLC. A fast reset
343 temporarily fixed the issue, but a reprogramming was required to properly resolve the issue. The
344 mean salinity offset during this time ranged from -7.0 to -2.5 (Fig. 4) compared to the set value
345 of c.a. -4.5, which was the primary contributor to the final value for the standard deviation (SD).

346 The main cause of temporary, but frequent, setpoint deviations larger than the mean value
347 was due to low flow rates (Fig. A6). Stochastically throughout the experiment, flow rates
348 averaging 7 to 8 L min⁻¹ would vary as a result of partial clogging, concomitant use of header
349 tank water from other parties in the marine lab, or occasional communication errors leading to
350 erroneous temperature setpoints that increased the ambient or heated seawater flow in a
351 mesocosm to outpace the filling of the respective header tanks. These instances were few,
352 however, and were not a result of the programmed control regulation of the SalTexPreS. Several
353 deviations > 2.0 salinity or °C could be explained by flow rates dropping to values < 2 L min⁻¹
354 (Fig. 4, 5). These low flow rates accounted for ~ 20 % of the large deviations in temperature and
355 salinity regulation. Occasions when flow rates were < 2 L min⁻¹ appeared to be minor in duration
356 and typically self-resolved (Fig. A6).

357 When accounting for the various incidences of improper regulation, the SalTexPreS was
358 able to simultaneously regulate 12 mesocosms comprised of 4 different conditions (1 control and
359 3 treatments) with an accuracy that deviated > 0.5 °C or 0.5 in salinity from the setpoint ≤ 20 %
360 and ≤ 30 % of the time, respectively, when flow rates were above 2 L min⁻¹ and excluding the
361 period of 90 m pump use (Fig. 5). Due to an erroneous control value during the 90 m usage,
362 these times were excluded. The % time deviation from a temperature setpoint > 1 °C reduced to
363 < 11 % for all treatments, and ≤ 20 % for all salinity treatments with the exception of the 1st



364 replicate for treatment 2. Regulation of temperature resulted in a higher accuracy than regulation
365 over salinity. This higher accuracy was trivial, however, as the average difference between
366 temperature and salinity accuracy as % time > 0.5 was ~ 1.5 % higher for temperature when
367 excluding the 1st replicate for treatment 2.

368
369 **Discussion**
370

371 The inaugural application of the fully autonomous SalTEPreS demonstrated the capacity for
372 this system to be successfully utilized for conducting *in situ* experiments on organisms or
373 communities exposed to multiple environmental drivers with a very good stability of treatment
374 conditions and an excellent match of the real-time natural variability. The versatility of the
375 system not only permits the manipulation of temperature and salinity, but could incorporate other
376 factors such as CO₂ or nutrient concentrations (Gazeau et al., *in prep*). The automated
377 component of the system can reduce logistical hurdles needed to perform high precision
378 replication and regulation of experimental conditions that track real-time system variability.
379 While the use of such a system can reduce user oversight and limitations, there is still a need for
380 diligent handling.

381 Some of the operational challenges encountered during the 2-month experiment in
382 Svalbard were able to be mitigated or resolved henceforth. The use of pop-up alert windows
383 when a lapse in connection occurred, or when data is not logging, along with secondary coding
384 instructions (as fail-safe instructions) ensuring that the last received *in situ* data were maintained
385 are examples how improvements made during the experiment facilitate a more robust
386 deployment for the future. These improvements are now incorporated into the available code for
387 programming of the SalTEPreS. These new editions were implemented during a second



388 deployment that occurred in the summer of 2022 under a similar experimental design, and
389 resulted in fewer lapses and frequencies of mis-regulation (Fig. 6). Further, we forewent
390 attempting to regulate the control condition (i.e., mixing chilled seawater with ambient to
391 account for unintended warming during transit from fjord to header tank to mesocosm) during
392 this second deployment as transit time and distance from pumped fjord water was substantially
393 less than this first application. The result of this decision was the complete resolution of
394 connection issues that regulate the control setpoint. As for some of the more common disruptions
395 that can occur during long-term experimental setups using raw seawater such as pump failure
396 and clogging, both of which impacted the performance of the SalTexPreS, were extraneous
397 instances that are not relevant to its direct performance. Other issues such as a sudden glitch in
398 the programming which resulted in a sudden freshening on 2021-08-03 07:30 UTC, or the
399 persistent miscommunication with the treatment 2 branched-PLC from 2021-07-26 to 2021-08-
400 03 UTC, could have been reduced by more fastidious monitoring of the SalTexPreS regulation.
401 We note that some of these issues were easily resolvable by resetting the Head PLC or cycling
402 the power of the system. In short, efficient user operation could further reduce deviations and
403 increase the accuracy of the SalTexPreS regulation.

404 This first and initial deployment of the SalTexPreS used to conduct a multi-stressor
405 experiment provided robust results for determining mixed kelp community metabolic responses
406 to future Arctic conditions (Miller et al., *in prep*). Many research endeavors and implementations
407 by the SalTexPreS have the potential to conduct a larger range of experimental settings that
408 pertain to environmental perturbation associated with climate change or other anthropogenic
409 forcings. The operational data produced are reliable, easily quantifiable, and provide the highest
410 degree of frequency for the monitoring of experimental conditions. The operation of such a



411 system in extreme environmental conditions has shown the durability of the manifold to endure
412 an adverse Arctic summer and still respond without mechanical failures. With proper operation
413 and user proficiency, this proves to be a highly sophisticated and powerful tool to be utilized for
414 aquatic perturbation experiments.

415 **Data availability**

416 The recorded parameters presented in this paper will be posted to Pangea and are available for
417 access.

418 **Acknowledgements**

419 This study is part of the FACE-IT Project (The Future of Arctic Coastal Ecosystems –
420 Identifying Transitions in Fjord Systems and Adjacent Coastal Areas). The authors thank Philipp
421 Fischer for access to the AWIPEV data as well as AWIPEV and Kings Bay staff for helping with
422 logistical details, shipping, and access to marine lab facilities.

423

424 **Author contributions**

425 C.M. and F.G. conceptualized the frame of the paper while F.G, S.C, and P.U. designed the
426 experimental system. C.M. wrote the manuscript and constructed the data analysis figures and
427 tables while P.U. designed the diagram figures. All authors revised, commented, and edited
428 during revision.

429

430 **Financial support**

431 FACE-IT has received funding from the European Union’s Horizon 2020 research and
432 innovation programme under grant agreement no. 869154. Partial financial support was provided
433 by IPEV, The French Polar Institute.



434

435 **Competing interest**

436 The authors declare no competing interests exist.

437

438 **References**

- 439 Bartsch, I., Paar, M., Fredriksen, S., Schwanitz, M., Daniel, C., Hop, H., and Wiencke, C.:
440 Changes in kelp forest biomass and depth distribution in Kongsfjorden, Svalbard, between 1996–
441 1998 and 2012–2014 reflect Arctic warming, *Polar Biol*, 39, 2021–2036,
442 <https://doi.org/10.1007/s00300-015-1870-1>, 2016.
- 443 Bass, A., Wernberg, T., Thomsen, M., and Smale, D.: Another Decade of Marine Climate
444 Change Experiments: Trends, Progress and Knowledge Gaps, *Frontiers in Marine Science*, 8,
445 2021.
- 446 Bhatia, M. P., Kujawinski, E. B., Das, S. B., Breier, C. F., Henderson, P. B., and Charette, M. A.:
447 Greenland meltwater as a significant and potentially bioavailable source of iron to the ocean,
448 *Nature Geosci*, 6, 274–278, <https://doi.org/10.1038/ngeo1746>, 2013.
- 449 Bindoff N. L., Cheung W. W. L., Kairo J. G., Arístegui J., Guinder V. A., Hallberg R., Hilmi N.,
450 Jiao N., Karim M. S., Levin L., O'Donoghue S., Purca Cuicapusa S. R., Rinkevich B., Suga T.,
451 Tagliabue A. & Williamson P., 2019. Changing ocean, marine ecosystems, and dependent
452 communities. In: Pörtner H.-O., Roberts D., Masson-Delmotte V. & Zhai P. (Eds.), *Special*
453 *Report on Ocean and Cryosphere in a Changing Climate*, pp. 447–587. Cambridge: Cambridge
454 University Press.
- 455
- 456 Blois, J. L., Williams, J. W., Fitzpatrick, M. C., Jackson, S. T., and Ferrier, S.: Space can
457 substitute for time in predicting climate-change effects on biodiversity, *Proc Natl Acad Sci U S*
458 *A*, 110, 9374–9379, <https://doi.org/10.1073/pnas.1220228110>, 2013.
- 459 Divya, D. T. and Krishnan, K. p.: Recent variability in the Atlantic water intrusion and water
460 masses in Kongsfjorden, an Arctic fjord, *Polar Science*, 11, 30–41,
461 <https://doi.org/10.1016/j.polar.2016.11.004>, 2017.
- 462 Evans, W., Mathis, J. T., Ramsay, J., and Hetrick, J.: On the frontline: Tracking ocean
463 acidification in an Alaskan shellfish hatchery, *PLOS ONE*, 10, e0130384,
464 <https://doi.org/10.1371/journal.pone.0130384>, 2015.
- 465 Fairchild, W. and Hales, B.: High-Resolution Carbonate System Dynamics of Netarts Bay, OR
466 From 2014 to 2019, *Frontiers in Marine Science*, 7, 2021.



- 467 Gattuso, J.-P., Alliouane, S., and Fischer, P.: High-frequency, year-round time series of the
468 carbonate chemistry in a high-Arctic fjord (Svalbard), *Earth System Science Data Discussions*,
469 1–24, <https://doi.org/10.5194/essd-2023-92>, 2023.
- 470 Hales, B., Suhrbier, A., Waldbusser, G. G., Feely, R. A., and Newton, J. A.: The Carbonate
471 Chemistry of the “Fattening Line,” Willapa Bay, 2011–2014, *Estuaries and Coasts*, 1–14,
472 <https://doi.org/10.1007/s12237-016-0136-7>, 2016.
- 473 Hop, H., Wiencke, C., Vögele, B., and Kovaltchouk, N. A.: Species composition, zonation, and
474 biomass of marine benthic macroalgae in Kongsfjorden, Svalbard, *Botanica Marina*, 55, 399–
475 414, <https://doi.org/10.1515/bot-2012-0097>, 2012.
- 476 Kroeker, K. J., Kordas, R. L., and Harley, C. D. G.: Embracing interactions in ocean
477 acidification research: confronting multiple stressor scenarios and context dependence, *Biology*
478 *Letters*, 13, 20160802, <https://doi.org/10.1098/rsbl.2016.0802>, 2017.
- 479 Kroeker, K. J., Bell, L. E., Donham, E. M., Hoshijima, U., Lummis, S., Toy, J. A., and Willis-
480 Norton, E.: Ecological change in dynamic environments: Accounting for temporal environmental
481 variability in studies of ocean change biology, *Global Change Biology*, 26, 54–67,
482 <https://doi.org/10.1111/gcb.14868>, 2020.
- 483 Meredith, M., Sommerkon, M., Cassotta, S., Derksen, C., Ekaykin, A., Hollowed, A., Kofinas,
484 G., Mackintosh, A., Melbourne-Thomas, J., Muelbert, M. M. C., Ottersen, G., Pritchard, H., and
485 Schuur, E. A. G.: Chapter 3: Polar regions — Special Report on the Ocean and Cryosphere in a
486 Changing Climate, IPCC, 2019.
- 487 Miller, C. A. and Kelley, A. L.: Seasonality and biological forcing modify the diel frequency of
488 nearshore pH extremes in a subarctic Alaskan estuary, *Limnology and Oceanography*, 66, 1475–
489 1491, <https://doi.org/10.1002/lno.11698>, 2021.
- 490 Olariaga, A., Guallart, E. F., Fuentes, V., López-Sanz, À., Canepa, A., Movilla, J., Bosch, M.,
491 Calvo, E., and Pelejero, C.: Polyp flats, a new system for experimenting with jellyfish polyps,
492 with insights into the effects of ocean acidification, *Limnology and Oceanography: Methods*, 12,
493 212–222, <https://doi.org/10.4319/lom.2014.12.212>, 2014.
- 494 Orr, J. A., Vinebrooke, R. D., Jackson, M. C., Kroeker, K. J., Kordas, R. L., Mantyka-Pringle,
495 C., Van den Brink, P. J., De Laender, F., Stoks, R., Holmstrup, M., Matthaei, C. D., Monk, W.
496 A., Penk, M. R., Leuzinger, S., Schäfer, R. B., and Piggott, J. J.: Towards a unified study of
497 multiple stressors: divisions and common goals across research disciplines, *Proceedings of the*
498 *Royal Society B: Biological Sciences*, 287, 20200421, <https://doi.org/10.1098/rspb.2020.0421>,
499 2020.
- 500 Overland, J., Dunlea, E., Box, J. E., Corell, R., Forsius, M., Kattsov, V., Olsen, M. S., Pawlak, J.,
501 Reiersen, L.-O., and Wang, M.: The urgency of Arctic change, *Polar Science*, 21, 6–13,
502 <https://doi.org/10.1016/j.polar.2018.11.008>, 2019.



- 503 Paar, M., de la Vega, C., Horn, S., Asmus, R., and Asmus, H.: Kelp belt ecosystem response to a
504 changing environment in Kongsfjorden (Spitsbergen), *Ocean & Coastal Management*, 167, 60–
505 77, <https://doi.org/10.1016/j.ocecoaman.2018.09.003>, 2019.
- 506 Pansch, C. and Hiebenthal, C.: A new mesocosm system to study the effects of environmental
507 variability on marine species and communities, *Limnology and Oceanography: Methods*, 17,
508 145–162, <https://doi.org/10.1002/lom3.10306>, 2019.
- 509 Poloczanska, E. S., Burrows, M. T., Brown, C. J., García Molinos, J., Halpern, B. S., Hoegh-
510 Guldberg, O., Kappel, C. V., Moore, P. J., Richardson, A. J., Schoeman, D. S., and Sydeman, W.
511 J.: Responses of Marine Organisms to Climate Change across Oceans, *Frontiers in Marine*
512 *Science*, 3, 2016.
- 513 Rastrick, S. S. P., Graham, H., Azetsu-Scott, K., Calosi, P., Chierici, M., Fransson, A., Hop, H.,
514 Hall-Spencer, J., Milazzo, M., Thor, P., and Kutti, T.: Using natural analogues to investigate the
515 effects of climate change and ocean acidification on Northern ecosystems, *ICES Journal of*
516 *Marine Science*, 75, 2299–2311, <https://doi.org/10.1093/icesjms/fsy128>, 2018.
- 517 Tverberg, V., Skogseth, R., Cottier, F., Sundfjord, A., Walczowski, W., Inall, M. E., Falck, E.,
518 Pavlova, O., and Nilsen, F.: The Kongsfjorden Transect: Seasonal and Inter-annual Variability in
519 Hydrography, in: *The Ecosystem of Kongsfjorden, Svalbard*, edited by: Hop, H. and Wiencke,
520 C., Springer International Publishing, Cham, 49–104, [https://doi.org/10.1007/978-3-319-46425-](https://doi.org/10.1007/978-3-319-46425-1_3)
521 [1_3](https://doi.org/10.1007/978-3-319-46425-1_3), 2019.
- 522 Wake, B.: Experimenting with multistressors, *Nat. Clim. Chang.*, 9, 357–357,
523 <https://doi.org/10.1038/s41558-019-0475-z>, 2019.
- 524 Ziegler, J. G. and Nichols, N. B.: Optimum Settings for Automatic Controllers, *Transactions of*
525 *the American Society of Mechanical Engineers*, 64, 759–765, <https://doi.org/10.1115/1.4019264>,
526 1943.
- 527
- 528
- 529
- 530
- 531
- 532
- 533
- 534



535 **Tables**

536 **Table 1.** Experimental treatments with given temperature and calculated salinity offsets based on
537 linear correlation with temperature (Fig. A1).

<i>Treatment</i>	<i>Temperature</i>	<i>Salinity</i>	<i>PAR</i>
Control	Ambient	Ambient	Ambient
Trt 1	+ 3.3 °C	$\Delta 2.5 - 3.0$ $y = 0.546 * T + 0.490$	~ 30% decrease from ambient
Trt 2	+ 5.3 °C	$\Delta 5.0 - 5.5$ $y = 0.877 * T + 0.089$	~ 50% decrease from ambient
Trt 3	+ 5.3 °C	Ambient	Ambient

538

539

540

541

542

543

544

545

546

547

548

549

550

551

552

553



554 **Table 2.** Absolute mean difference between measured temperature and salinity against setpoints
 555 plus or minus the standard deviation. A weighted average was used for treatments 1 – 3 to
 556 account for the 5-day incremental increase. Cntrl. is the control and Trt. is treatment 1 – 3 with
 557 replicates a – c.

<i>Treatment</i>	<i>Mean diff</i>		<i>Manipulated water</i>			
	<i>Abs(T_{meas.} - T_{set})</i>	<i>Abs(S_{meas.} - S_{set})</i>	<i>Cold</i>	<i>Ambient</i>	<i>Warm</i>	<i>Fresh</i>
<i>Cntrl. a</i>	0.275 ± 0.39	–	x	x		
<i>Cntrl. b</i>	0.291 ± 0.36	–	x	x		
<i>Cntrl. c</i>	0.223 ± 0.36	–	x	x		
<i>Trt. 1a</i>	0.126 ± 0.31	0.116 ± 0.31		x	x	x
<i>Trt. 1b</i>	0.142 ± 0.29	0.148 ± 0.22		x	x	x
<i>Trt. 1c</i>	0.145 ± 0.33	0.171 ± 0.33		x	x	x
<i>Trt. 2a</i>	0.111 ± 0.29	0.357 ± 0.74		x	x	x
<i>Trt. 2b</i>	0.133 ± 0.29	0.149 ± 0.26		x	x	x
<i>Trt. 2c</i>	0.196 ± 0.38	0.128 ± 0.25		x	x	x
<i>Trt. 3a</i>	0.109 ± 0.27	–		x	x	
<i>Trt. 3b</i>	0.112 ± 0.27	–		x	x	
<i>Trt. 3c</i>	0.106 ± 0.28	–		x	x	

558

559

560

561

562

563

564

565

566

567

568

569

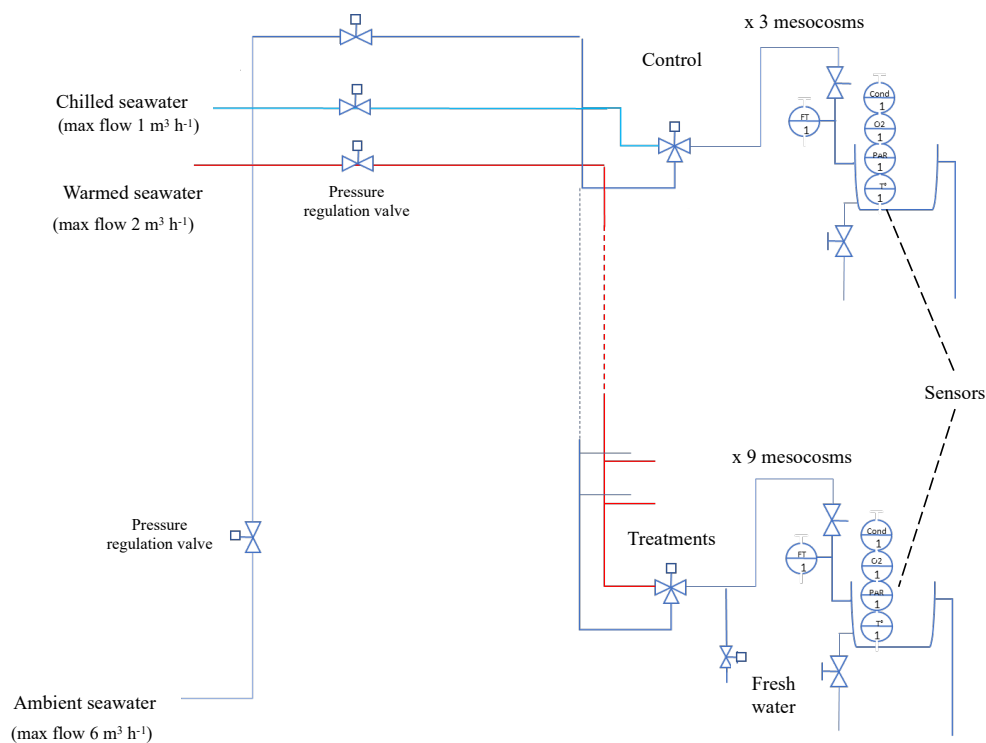
570

571



572 **Figures**

573



574

575 **Figure 1.** Piping schematic of mixing and regulation manifold for SalTExPreS.

576

577

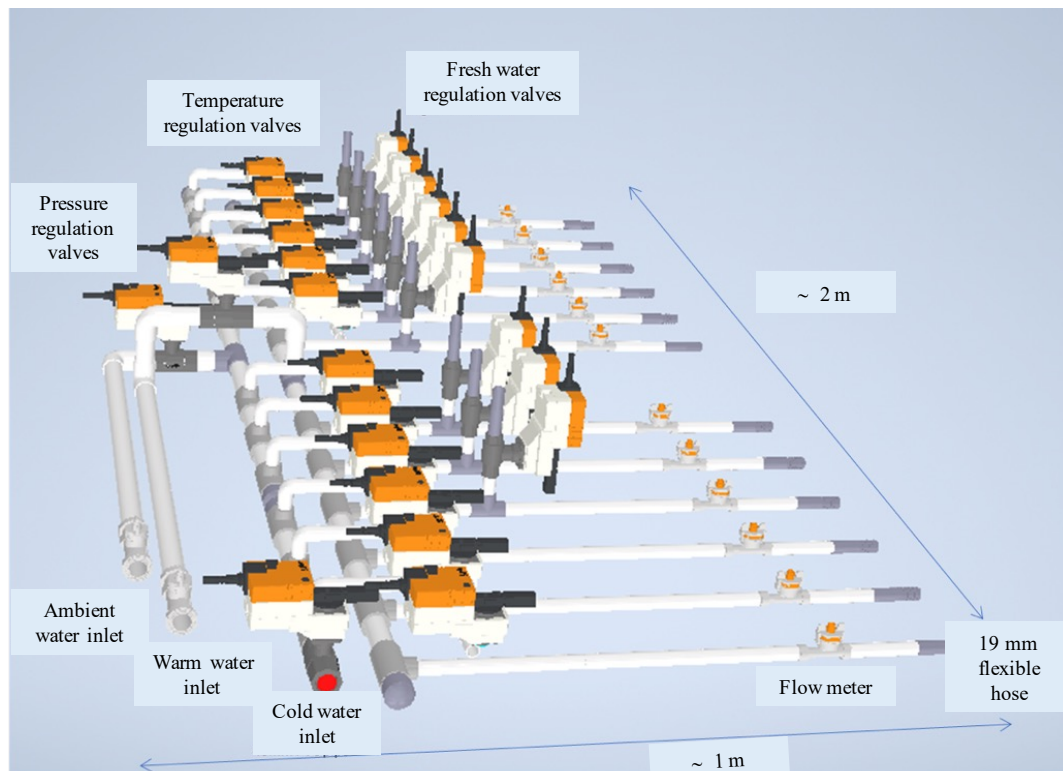
578

579

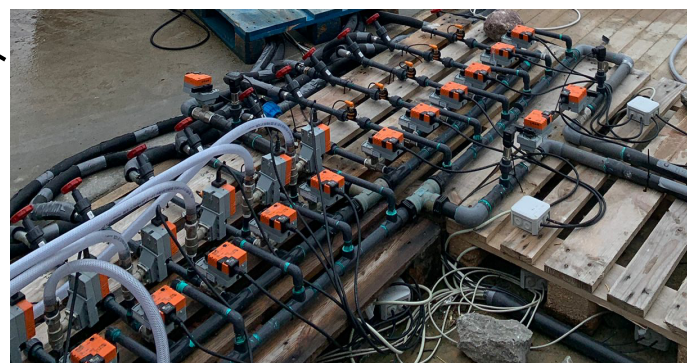
580

581

582



583



584

585

586 **Figure 2.** Visual diagram of manifold layout and actual application at the experimental site in

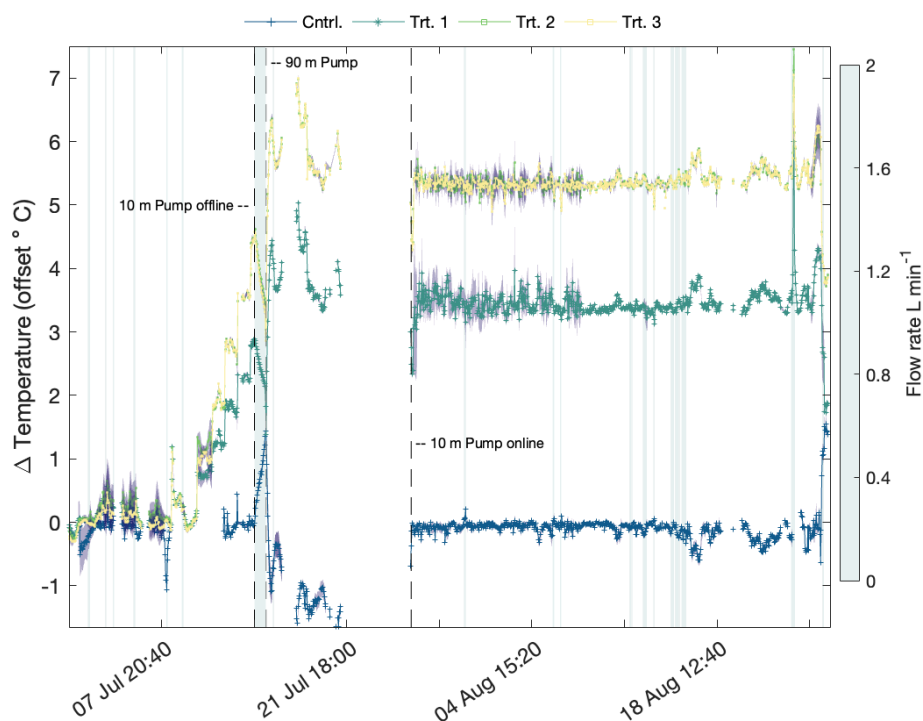
587 Ny-Ålesund, Svalbard.

588

589



590



591

592 **Figure 3.** Regulation of the temperature offset during the experimental period for the mean value

593 of all treatment conditions and ambient-control. The purple shaded region around the mean is the

594 standard deviation and the heatmap isoclines are the instances when flow rates $\leq 2 \text{ L min}^{-1}$.

595 Dashed black lines indicate periods when the pump at 10 m depth and 90 m depth were used to

596 feed header tanks.

597

598

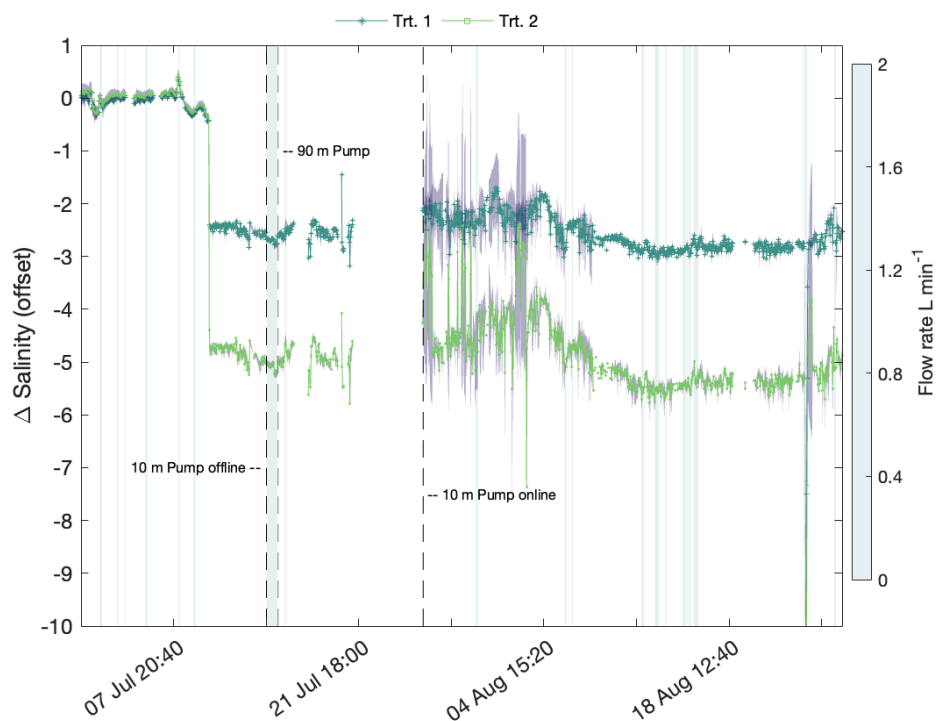
599

600

601



602



603

604 **Figure 4.** Regulation of the mean salinity offset (Δ salinity) during the experimental period for

605 treatments 1 and 2. The purple shaded region around the mean is the standard deviation and the

606 heatmap isoclines are the instances when flow rates $\leq 2 \text{ L min}^{-1}$. Dashed black lines indicate

607 periods when the pump at 10 m depth and 90 m depth were used to feed header tanks.

608

609

610

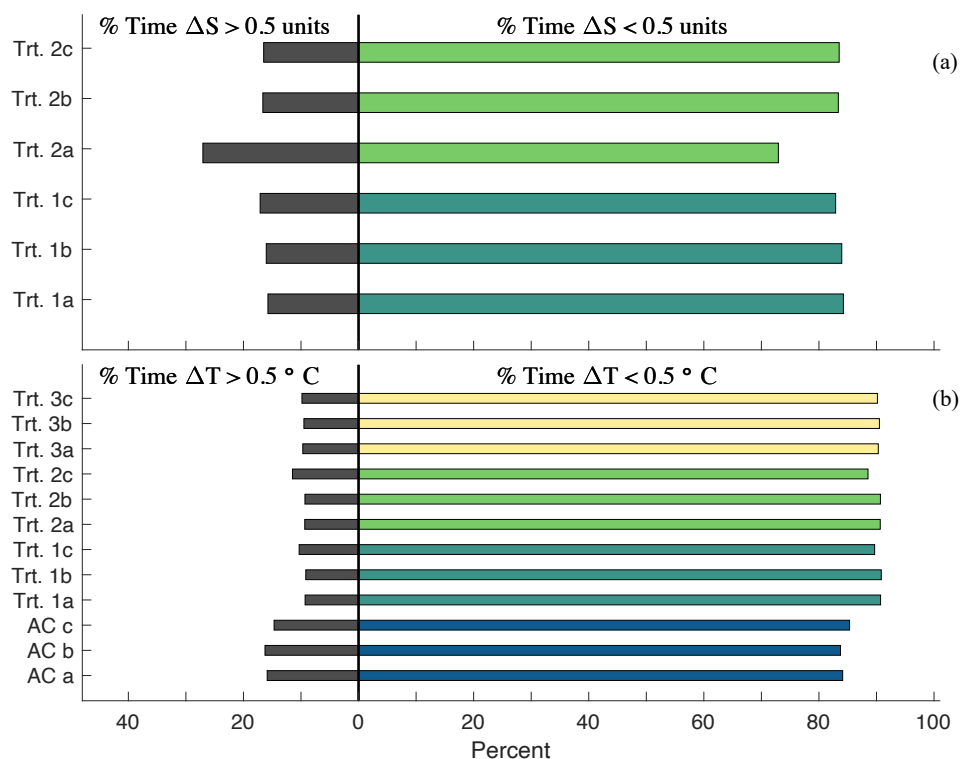
611

612

613



614



615

616 **Figure 5.** Percent time each mesocosm had a deviation $>$ (black bars) or $<$ (colored) 0.5 (ΔS ; **a**)

617 or 0.5 °C (ΔT ; **b**) when flow rates were above 2 L min⁻¹ spanning 42 days out of the 54 days of

618 the experiment: excluding the time when using the 90 m pump as regulation setpoints were

619 invalid due to an erroneous control.

620

621

622

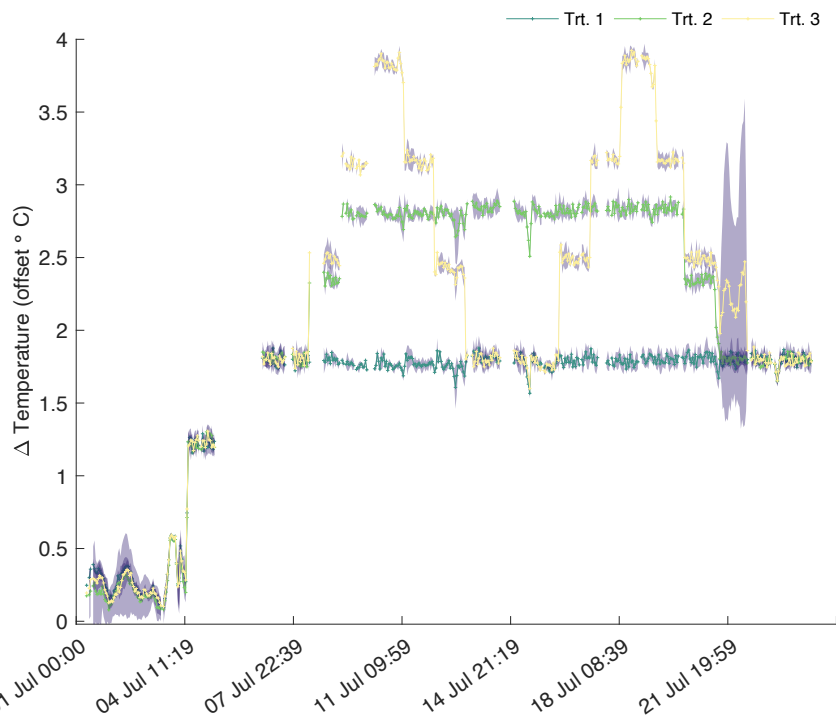
623

624

625



626



627

628 **Figure 6.** Regulation of the mean temperature offset (Δ temperature) during the 2nd deployment

629 of SalTExPreS in the summer of 2022 in Tromsø (Norway) performing a variation of heatwave

630 scenarios with three experimental treatments 1 – 3. The purple shaded region around the mean is

631 the standard deviation.

632

633

634

635

636

637

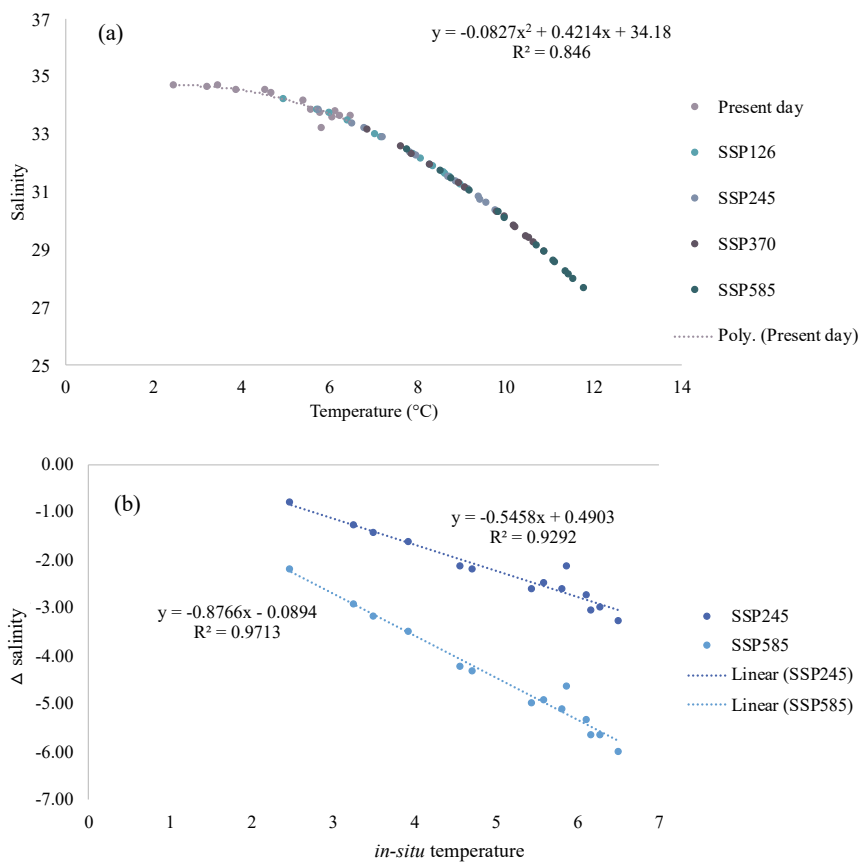
638



639 **Appendix A**

640 **Table A1.** Functions used for programming of software

Function	Operation	Auxiliary field Sender ID	Auxiliary field Command #
<i>RTC/read()</i>	The PLCs are equipped with a RTC chip and battery to keep track of the date. Once set on commissioning, RTC.read() returns the current date and time. This functions loops through each sensor connected on the RS485 bus. Each Mesocosm has two sensors (O2 and Conductivity/Salinity), so each PLC has 6 sensors connected on its bus.		
<i>readMesosensors()</i>	- O2 sensors have addresses ranging from 10 to 12, for mesocosms 0 to 2 of the scenario, respectively. - PC4E sensors have addresses ranging from 30 to 32, for mesocosms 0 to 2 of the scenario, respectively. - Sensors are requested individually and in sequence. A request is made every 200 ms.		
<i>websocket loop()</i>	This is a callback function responsible for dealing with the Websocket communication. The master PLC is the Websocket server. It listens to slave PLCs requests and to the monitoring PC requests. Requests are JSON formatted. They always contain <i>anctid/ty/fields</i> : sendatID (ID of the entity sending the request), conatID (ID of the requested entity), command (command type of the request). They optionally can also contain a « time » field: Unix-like timestamp (number of seconds since 01-01-1970)	Head PLC (ID = 0) Branch PLCs (ID = 1-3) Monitoring PC (ID = 4)	Request params: aspoints, PID settings (# = 0) Send Params: measurement values, regulation outputs (# = 1) Send Data: response to a « request params » request (# = 2) Calibrate sensor: request for calibrating sensor to specified value (# = 4) Request Head data: specific data measured by Head PLC (pressure & flow rates) (# = 5) Send Head data: a response to a « request Head data » request (# = 6)
<i>regulationTemperature()</i>	This function is responsible for the temperature regulation of the mesocosm. It sets the corresponding three-way valve position using a 0-10V analog signal. The function first checks if the regulation is in « manual override » mode. If so, it applies the override setpoint. If not, it reads the temperature measure in the mesocosm, compares it with the setpoint, and uses the PID settings to set the valve position.		
<i>checkMesocosms()</i>	This functions loops through every mesocosm every 200 ms and reads analog signals (i.e., flowrates and pressure readings).		
<i>regulationPressure()</i>	This function is responsible for the pressure regulation of the mesocosm. It sets the corresponding three-way valve position using a 0-10V analog signal. The function first checks if the regulation is in « manual override » mode. If so, it applies the override setpoint. If not, it reads the pressure measure in the mesocosm, compares it with the setpoint, and uses the PID settings to set the valve position.		
<i>printTASD()</i>	Master PLC is equipped with a microSD card, on which data from all mesocosms is logged every 5 seconds, in one csv file per day. This is for security only, as the microSD card is not easy to remove from the PLC casing. It should not be removed before the end of the experiment.		
<i>regulationSalinity()</i>	This function is responsible for the salinity regulation of the mesocosm. It sets the corresponding three-way valve position using a 0-10V analog signal. The function first checks if the regulation is in « manual override » mode. If so, it applies the override setpoint. If not, it reads the salinity measure in the mesocosm, compares it with the setpoint, and uses the PID settings to set the valve position.		



642

643

644 **Figure A1.** Relationship between temperature and salinity in summer 2020 weeks 22 – 35 in Ny-

645 Ålesund, Svalbard. **(a)** Relationship extrapolated using temperature offsets for projected 2100

646 SSP scenarios. **(b)** Applied salinity offsets based on relationship with temperature used for

647 treatments 1 and 2 (Table 1).

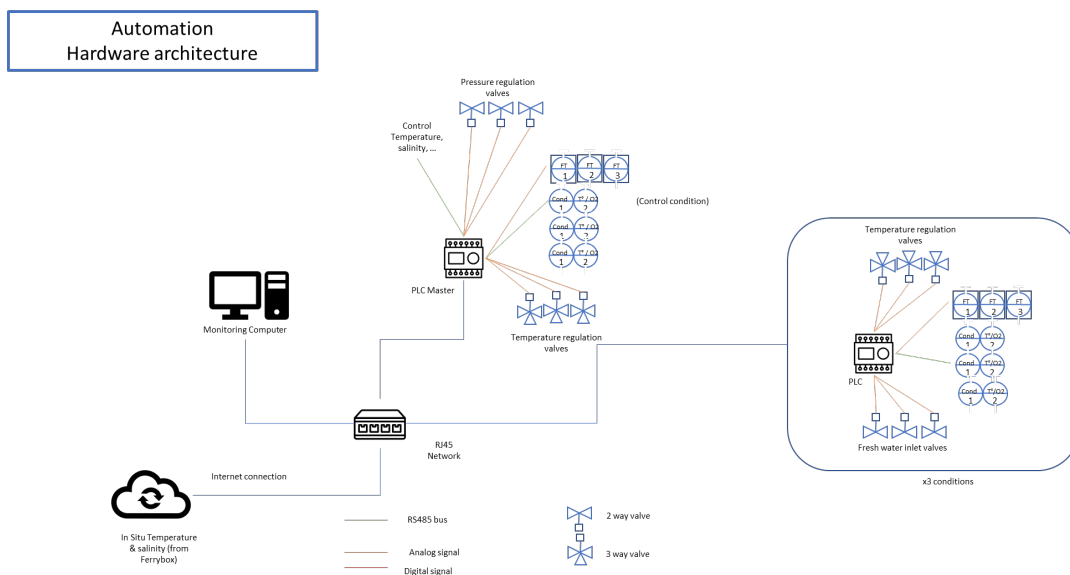
648

649

650

651

652



653

654 **Figure A2.** Diagram and flow-chart of the automation system.

655

656

657

658

659

660

661

662

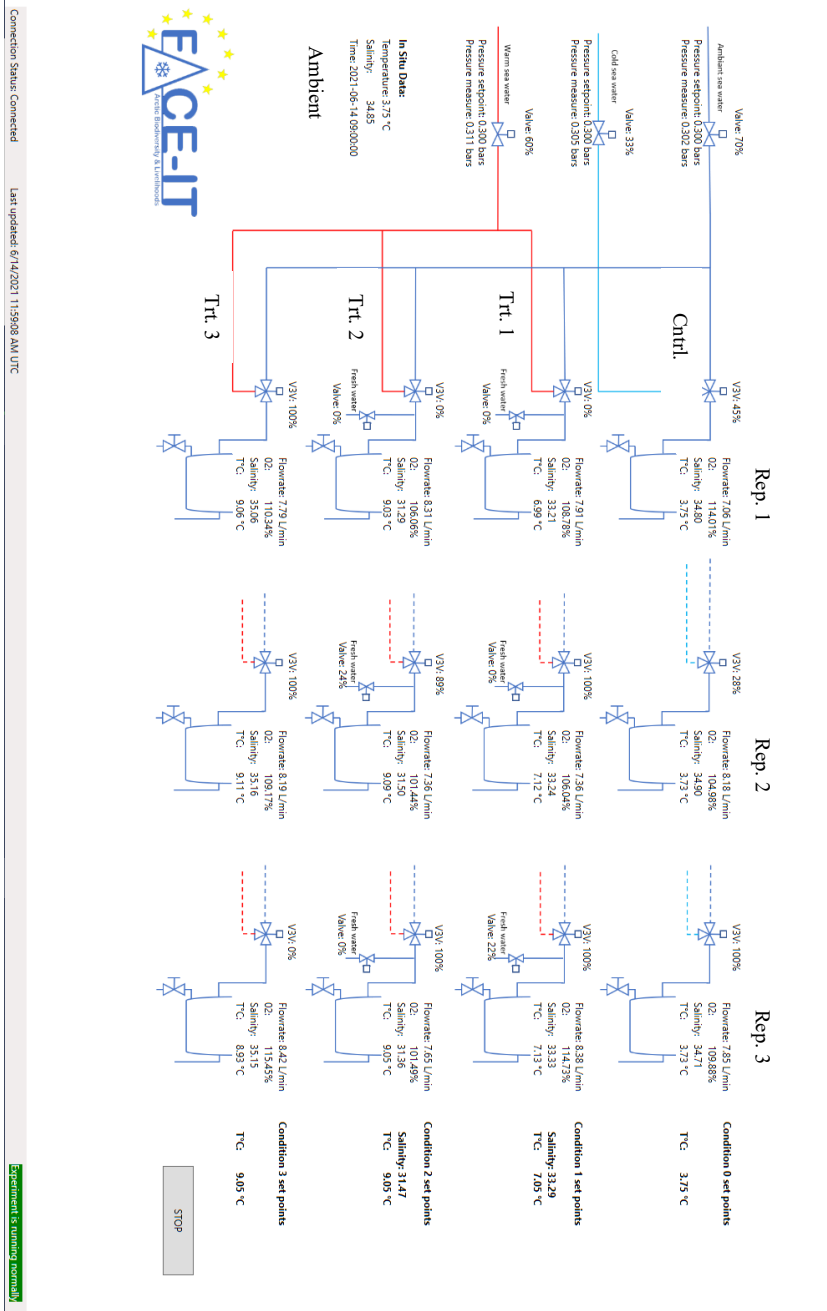
663

664

665

666

667



668

669 **Figure A3.** Application interface displaying real-time monitoring of ambient conditions as well
 670 and control (Cntl.), and treatment (Trt.) conditions for each replicate (Rep.) in each mesocosm.



672 **Figure A4.** Operation windows for the application and experimental settings (**a-c**). These
673 windows are found under the ‘settings’ tab. Operation windows for sensor calibration and
674 debugging (**d, e**). These are found under the ‘maintenance’ tab.

675

676

677

678

679

680

681

682

683

684

685

686

687

688

689

690

691

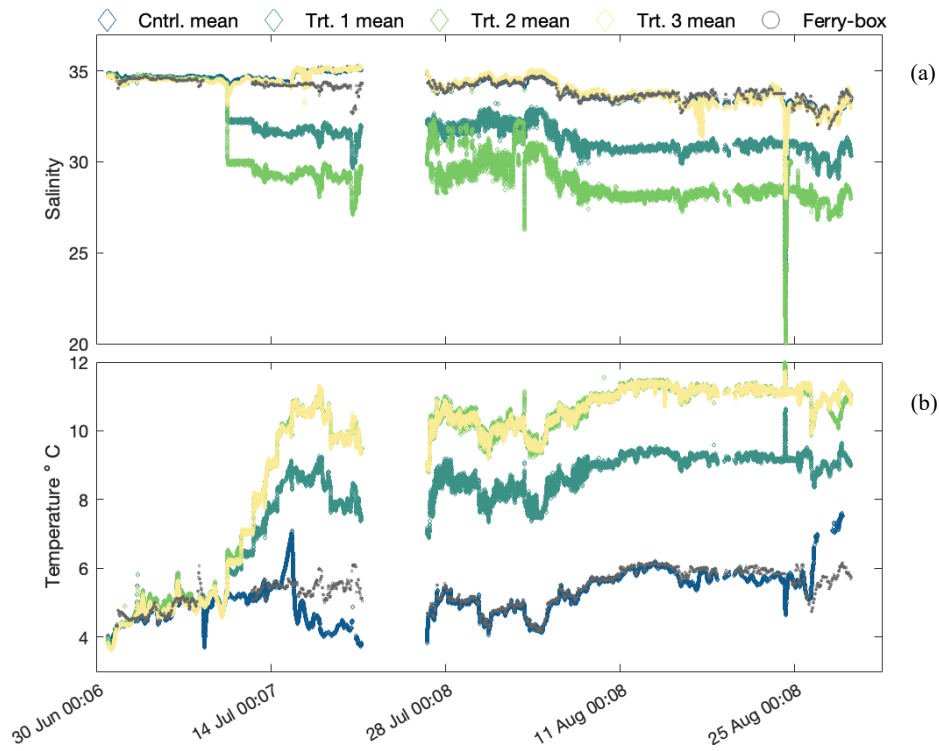
692

693

694



695



696

697 **Figure A5.** Mean temperature (a) and salinity (b) over the entire operation of the experimental

698 system.

699

700

701

702

703

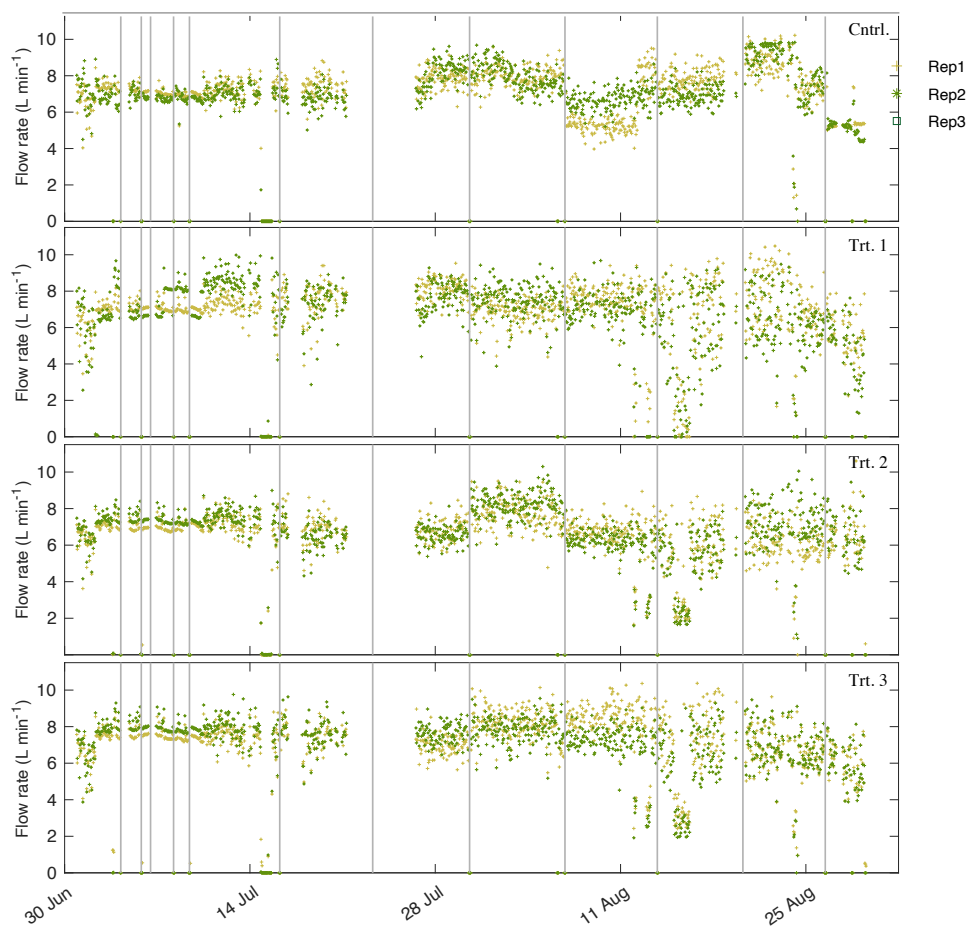
704

705

706



707



708

709 **Figure A6.** Flow rates for ambient-control, and treatments 1-3 for the entirety of the system

710 operation. Black isoclines are when incubations were performed and the system was shut-off for

711 a period of 3 h. Flow rates went to zero at these times.

712

713



714

715 **Figure A7.** Electrical cabinet used for SalTexPreS

716

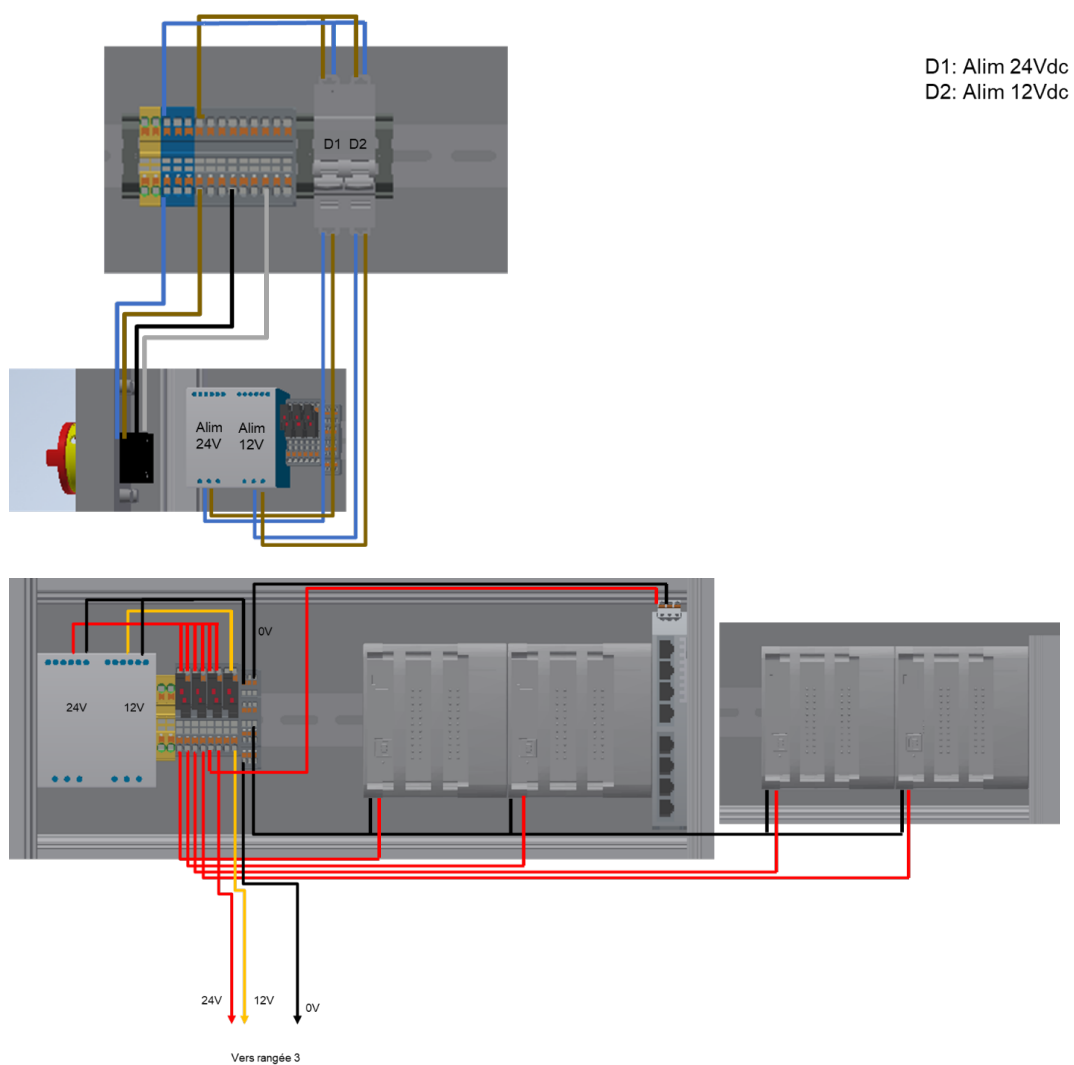
717

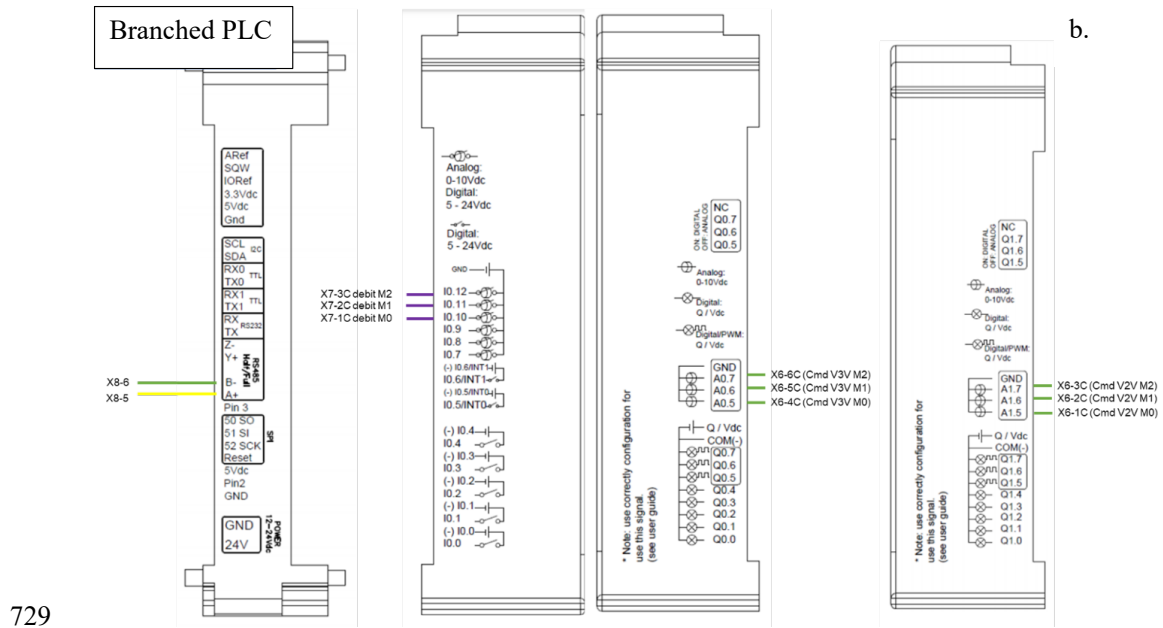
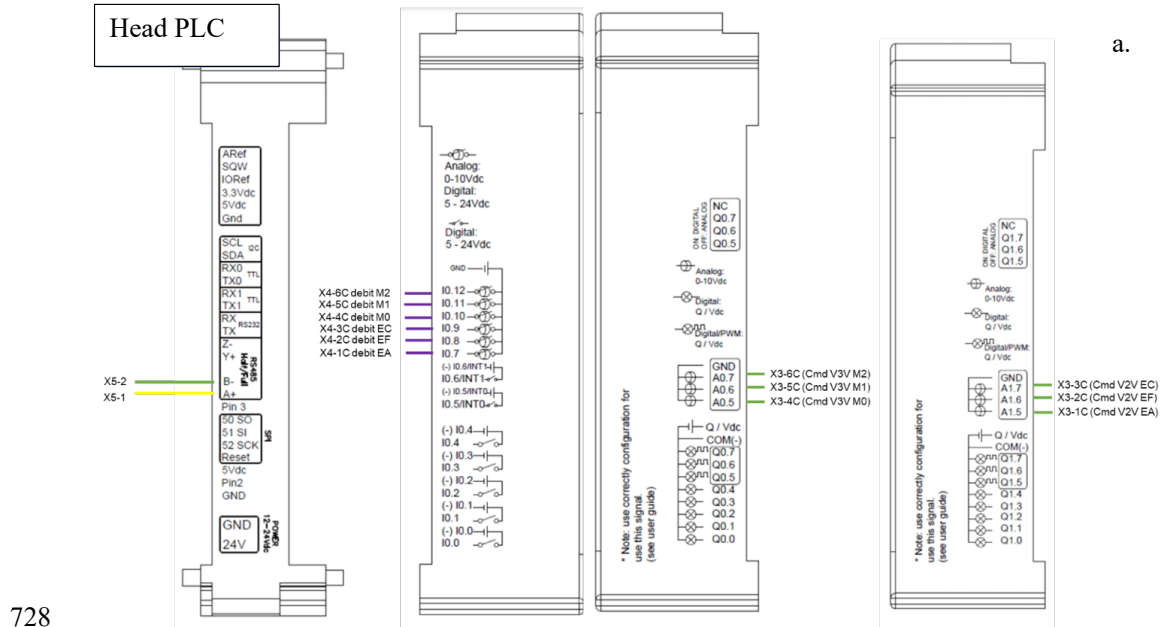
718

719



720 **Figure A8.** Electrical schematic for wiring within the electrical box.





730 **Figure A9.** PLC controller diagram for Head (a) and Branched (b) operations.

731

732



733 **Table A2. Parts list with manufacturer model numbers.**

Group	Item	Supplier/manufacturer	Model / details	Quantity
Hydraulic system				
	Mesocosms	home made	1000 L fiber glass	12
	Seawater pump	NPS	Albatros F13T	1
	PVC-U tubing and fittings		20mm, 32mm & 50mm diameter	–
	Insulated flexible hose		19mm diameter	100 m
Sensors				
	Conductivity / temperature	Aqualabo	PC4E	12
	Oxygen	Aqualabo	PODOC	12
	Pressure	Siemens	7MF1567-3BE00-1AA1	3
	Flow rate	IFM	SV3150	12
Actuators				
	Pressure regulation valves	BELIMO	R2025-10-S2 with LR24A-SR motor	3
	Temperature regulation valves	BELIMO	R3015-10-S2 with LR24A-SR motor	12
	Salinity regulation valves	BELIMO	R2015-10-S2 with LR24A-SR motor	6
Automation cabinet				
	Cabinet	Fibox	FIB8120017N	1
	Security switch	KRAUS-NAIMER	KNA002245	1
	12 vdc power supply	Lambda	LAMDRL30-12-1	1
	24vdc power supply	Lambda	LAMDRB240-24-1	1
	PLC	Industrial shields	Mduino-42+	4
	Ethernet switch	HIRSCHMANN-INET	HIR942132002	1

734